In-plane anisotropy in two-dimensional electron gas at $LaAlO_3/SrTiO_3(110)$ interface*

Sheng-Chun Shen(沈胜春), Yan-Peng Hong(洪彦鹏), Cheng-Jian Li(厉承剑), Hong-Xia Xue(薛红霞), Xin-Xin Wang(王欣欣), and Jia-Cai Nie(聂家财)†

Department of Physics, Beijing Normal University, Beijing 100875, *China*

(Received 24 November 2015; revised manuscript received 21 March 2016; published online 9 June 2016)

A systematic study of the two-dimensional electron gas at $LaAlO_3/SrTiO_3(110)$ interface reveals an anisotropy along two specific directions, [001] and $[1\bar{1}0]$. The anisotropy becomes distinct for the interface prepared under high oxygen pressure with low carrier density. Angular dependence of magnetoresistance shows that the electron confinement is stronger along the $[1\bar{1}0]$ direction. Gate-tunable magnetoresistance reveals a clear in-plane anisotropy of the spin–orbit coupling, and the spin relaxation mechanism along both directions belongs to D'yakonov–Perel' (DP) scenario. Moreover, in-plane anisotropic superconductivity is observed for the sample with high carrier density, the superconducting transition temperature is lower but the upper critical field is higher along the $[1\bar{1}0]$ direction. This in-plane anisotropy could be ascribed to the anisotropic band structure along the two crystallographic directions.

Keywords: oxide interfaces, two-dimensional electron gas, anisotropy

PACS: 68.47.Gh, 73.20.–r, 81.15.Fg **DOI:** 10.1088/1674-1056/25/7/076802

1. Introduction

Two-dimensional electron gas (2DEG) formed at the interface between two band insulators $LaAlO_3$ (LAO) and $SrTiO_3$ (STO) exhibits many fascinating properties, such as magnetism,[1] superconductivity,[2,3] and their coexistence.[4–6] Besides, the observation of the spin–orbit coupling (SOC) in this system provides possibilities to control the orbital motion of electrons by acting on their spins.[7–9] Initially, the vast majority of the investigations were specific only to the LAO/STO(001) interfaces.[1–10] However, recent findings have shown that 2DEGs can be formed at interfaces with different crystal orientations, such as LAO/STO(110).[11,12] and LAO/STO(111),[12] opening fresh perspectives to understand the fundamental physics and to offer new functionalities.

Via x-ray linear dichroism spectroscopy, Pesquera *et al.* recently demonstrated an intrinsic distinctive electronic structure of the 2DEG at the LAO/STO(110) interface due to the different orbital symmetry and hierarchy compared to those of the (001)-oriented interface.[13] Therefore, the physical properties, such as superconductivity and SOC,[14–17] could be influenced by the distinctive orbital symmetry and hierarchy. Latest studies on the LAO/STO(110) interfaces revealed distinct superconductivity and Rashba SOC,[16] and the SOC is insensitive to the gate voltage owing to the stronger polarizations of d_{xy}, d_{yz}/d_{zx} orbitals along the confinement direction. Moreover, for the LAO/STO(110) interface, there are two different crystal directions, i.e., [001] and $[1\bar{1}0]$, in the plane of the interface. Recent angle-resolved photoemission (ARPES) studies on $SrTiO_3(110)$ surface showed a high electronic in-plane anisotropy along the two specific directions, and the anisotropy is pronounced at lower carrier density when only d_{yz}/d_{zx}-derived ellipsoids are occupied.[18] Hence, the in-plane crystallographic directions of LAO/STO(110) may offer an extra degree of freedom to tune the properties of 2DEG. A few of the latest works mentioned the existence of the in-plane anisotropy,[11,17] however a systematic study of the in-plane anisotropy in the (110) system is still required. Here, we present a careful and systematic research of the influence of the crystallographic direction on both normal state and superconducting properties at the LAO/STO(110) interfaces.

2. Experimental method

The samples with ten unit cells of LAO were grown at two different oxygen partial pressures (P_{O2}), 10^{-4} Torr and 10^{-3} Torr, on treated (110)-oriented $SrTiO_3$ substrates by pulsed laser deposition. The details of the growth procedure have been given in Ref. [15]. After preparation, two Hall bar structures were patterned in the same sample by using a standard photolithography technique, the LAO layers and a few STO layers were removed by low energy argon ion milling. For the directional dependence magnetotransport measurements, the Hall bar structures were along [001] and $[1\bar{1}0]$ crystallographic directions, respectively. An etched STO surface was insulating, indicating that the conducting channels

*Project supported by the Ministry of Science and Technology of China (Grant Nos. 2013CB921701, 2013CBA01603, and 2014CB920903), the National Natural Science Foundation of China (Grant Nos. 10974019, 51172029, 91121012, 11422430, 11374035, 11474022, and 11474024), the Program for New Century Excellent Talents in the University of the Ministry of Education of China (Grant No. NCET-13-0054), and the Beijing Higher Education Young Elite Teacher Project, China (Grant No. YETP0238).

†Corresponding author. E-mail: jcnie@bnu.edu.cn

© 2016 Chinese Physical Society and IOP Publishing Ltd

were at the interfaces. Ohmic contacts between electrode pad and sample interface were made by wire bonding. Magnetotransport properties were measured at temperature $T = 2$ K and with a magnetic field up to 9 T by a commercial Physical Properties Measurement System (Quantum Design, PPMS) equipped with a rotating sample holder. The gate was applied to the backside of the $SrTiO_3$ substrate by a voltage source and no leakage current (< 1 nA) was detected for ± 100 V gate voltages (V_G).

3. Results and discussion

The anisotropic out-of-plane magnetoresistance (MR) along two directions, $[1\bar{1}0]$ and [001], is shown in Fig. 1. The MR is defined as $\Delta R/R_0 = [R(B) - R(B=0)]/R(B=0)$, where $R(B)$ is the sheet resistance in the magnetic field B. As we can see from Fig. 1(a), for the sample prepared at $P_{O2} \sim 10^{-4}$ Torr, the MR linearly increases with increasing magnetic field for both directions. The anisotropy is not obvious; but for the interface prepared at $P_{O2} \sim 10^{-3}$ Torr, the anisotropy of the MR becomes obvious, as shown in Fig. 1(b). Along the $[1\bar{1}0]$ direction, the MR firstly increases and then decreases with increasing magnetic field. These results indicate that the anisotropy along the two directions is pronounced at lower carrier density, which is consistent with the ARPES results on the STO(110) surface, attributed to the occupation of orbitals.[18] In order to effectively exploit the anisotropy of the 2DEG at the LAO/STO(110) interface, we now focus on the sample prepared at high P_{O2} (10^{-3} Torr) with a relatively low carrier density.

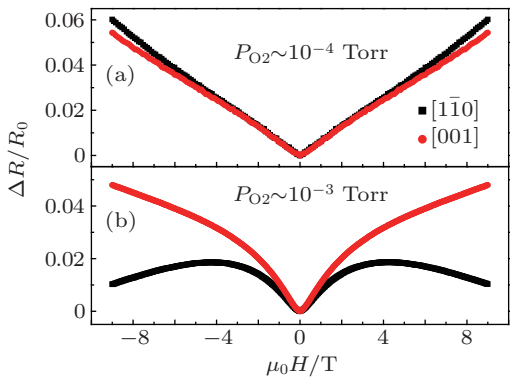


Fig. 1. (color online) The magnetoresistance measured along $[1\bar{1}0]$ (black) and [001] (red) directions of LAO/STO(110) for samples prepared under oxygen partial pressures of (a) 10^{-4} Torr and (b) 10^{-3} Torr.

Anisotropic MR was investigated for different angle θ between the direction of the interface normal and the magnetic field. For the investigation of angular MR, the magnetic field was rotated from out-of-plane ($\theta = 0°$, i.e., perpendicular to the surface) to in-plane ($\theta = 90°$, parallel to the current) at 2 K. As shown in Fig. 2(a), along the $[1\bar{1}0]$ direction, as the magnetic field increases, the MR gradually increases in the low field regime and then starts to decrease in the higher field. There is a local MR maximum, a positive slope in the low magnetic field regime but a negative slope in the high magnetic field regime. Besides, a negative MR appears for $\theta > 60°$ and the negative MR regime widens out as θ increases. Moreover, with increasing θ, the maximum of the MR slightly shifts to low magnetic field and the value becomes smaller. Along the [001] direction, the MR decreases as θ increases from 0° to 90°; and the local MR maximum appears at large angles, as shown in Fig. 2(b). The behavior of the in-plane MR is similar, while an obvious difference of MR along two directions can be observed at $\theta = 0°$ (perpendicular magnetic field), indicating that the anisotropy is more pronounced in the plane of the interface.

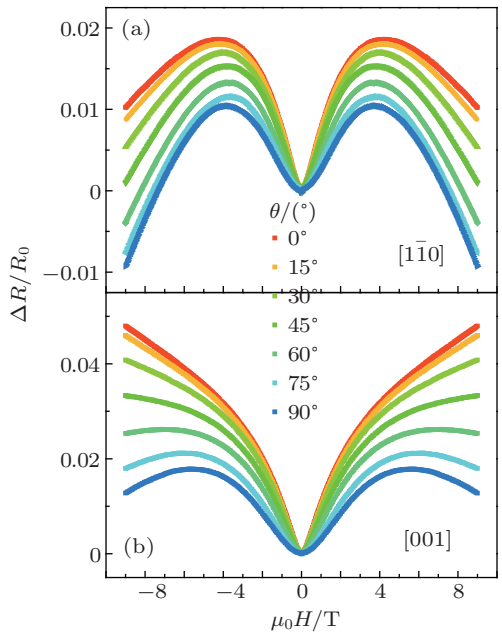


Fig. 2. (color online) The magnetoresistance for different angles θ along (a) $[1\bar{1}0]$ and (b) [001] directions.

The positive out-of-plane MR is attributed to the orbital effect, while the in-plane MR rules out this effect. The difference of out-of-plane MR between [001] and $[1\bar{1}0]$ directions suggests that crystallographic anisotropy plays a critical role in magnetotransport properties. The negative MR appears and becomes visible as the parallel magnetic field increases, as shown in Fig. 2. The negative MR can be counteracted by the positive contribution for the out-of-plane field case. When applying the parallel magnetic field, the suppression of positive MR indicates that the confinement zone of 2DEG is within one carrier mean free path. We assume that only one subband is occupied, then the mean-free path can be naively calculated by using formula $l = \frac{h}{e^2 k_F R_s}$,[19] where l is the mean-free path, h is the Planck constant, e is the electron charge, R_s is the sheet resistance, $k_F = \sqrt{2\pi n_s}$ is the Fermi wave number, and n_s is the carrier density. Then at $T = 2$ K, the mean-free path is found to be about 22 nm along the $[1\bar{1}0]$ direction, while it is about

34 nm along the [001] direction, the same order of magnitude compared with that reported by Ben Shalom *et al.* for (001)-orientation LAO/STO interfaces. It is noted that the mean-free path is shorter along the $[1\bar{1}0]$ direction than that of [001], suggesting that scattering becomes stronger along the $[1\bar{1}0]$ direction.

The remarkable angular dependence of MR and the appearance of negative MR indicate that the 2D weak localization effect should be considered. The magnetic field dependence of MR provides an important insight into the coupling between spin dynamics and transport. The existence of a local maximum MR and the appearance of a negative MR were also observed in other two-dimensional disordered systems,[20–22] which is associated with the weak localization related to the presence of spin–orbit interactions (weak antilocalization).[23–26] In LAO/STO heterostructures, the local electric field is enhanced by the accumulation of electrons in the interfacial quantum well, giving rise to the SOC. A strong spin–orbit field has been demonstrated at both (001) and (110)-oriented LAO/STO interfaces.[7,8,16,17]

For the investigation of directional dependence of SOC, we measured the MR as a function of V_G, as shown in Fig. 3. Due to the high dielectric constant of $SrTiO_3$,[27] the properties of 2DEG can be effectively tuned by a backgate voltage.[7,8] As shown in Fig. 3(a), the sheet resistances along two directions vary as V_G changes. Also the sheet resistance along the $[1\bar{1}0]$ direction is more sensitive to the applied electric field and is larger than that along the [001] direction. Figures 3(b) and 3(c) show the gate-tunable MR at different V_G along two directions. Along the $[1\bar{1}0]$ direction, the MR decreases with increasing V_G, the local MR maximum shifts to low magnetic field, while along the [001] direction, the local MR maximum appears only for negative V_G.

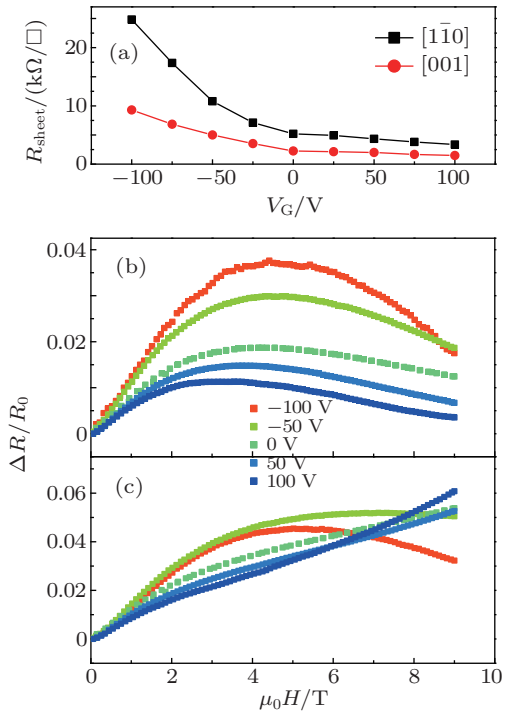


Fig. 3. (color online) (a) The sheet resistance as a function of V_G along two directions. The magnetoresistance at different V_G along (b) $[1\bar{1}0]$ and (c) [001] directions.

Table 1. Transport parameters along [001] direction.

V_G/V	R_{sheet}/(kΩ/□)	$n/10^{13}$ cm^{-2}	D/cm^2·s^{-1}	B_{SO}/T	B_ϕ/T	$\tau_{SO}/10^{-12}$ s	$\tau_\phi/10^{-12}$ s	$\tau/10^{-13}$ s
−100	9.30	2.21	0.54	1.30	0.54	2.37	5.73	0.52
−75	6.84	2.36	0.73	1.38	0.43	1.63	5.30	0.66
−50	5.00	2.51	1.00	1.44	0.35	1.15	4.73	0.85
−25	3.51	2.73	1.42	1.62	0.29	0.72	4.07	1.11
0	2.25	2.80	2.21	1.84	0.23	0.40	3.18	1.69
25	2.13	2.85	2.34	1.71	0.28	0.41	2.47	1.75
50	199	2.77	2.50	1.95	0.23	0.34	2.88	1.93
75	1.66	2.73	2.99	2.27	0.23	0.24	2.37	2.34
100	1.48	2.67	3.36	2.27	0.22	0.22	2.21	2.68

Table 2. Transport parameters along $[1\bar{1}0]$ direction.

V_G/V	R_{sheet}/(kΩ/□)	$n/10^{13}$ cm^{-2}	D/cm^2·s^{-1}	B_{SO}/T	B_ϕ/T	$\tau_{SO}/10^{-12}$ s	$\tau_\phi/10^{-12}$ s	$\tau/10^{-13}$ s
−100	24.82	3.73	0.20	1.17	0.85	7.03	9.65	0.11
−75	17.37	3.57	0.29	1.10	0.71	5.20	8.14	0.17
−50	10.79	3.22	0.46	1.03	0.58	3.45	6.13	0.31
−25	7.11	2.88	0.70	0.99	0.50	2.39	4.71	0.52
0	5.19	2.81	0.96	0.98	0.47	1.74	3.62	0.73
25	4.92	2.87	1.01	0.95	0.53	1.70	3.09	0.75
50	4.33	2.83	1.15	0.94	0.47	1.53	3.08	0.87
75	3.80	2.80	1.311.49	0.88	0.43	1.42	2.92	1.00
100	3.35	2.58		0.83	0.40	1.33	2.74	1.23

The conductance correction due to the weak localization is modified by the SOC. The influence of the SOC can therefore be assessed by properly analyzing the magnetoconductance in the diffusion regime. The magnetic field dependence of the conductance correction normalized by the quantum of conductance as a function of V_G is investigated, as shown in Fig. 4. We fit the experimental data by using the Maekawa–Fukuyama (MF) form[8,28]

$$\frac{\Delta\sigma(B)}{G_0} = \Psi\left(\frac{B}{B_\phi + B_{SO}}\right) + \frac{1}{2\sqrt{1-\gamma^2}}\Psi\left(\frac{B}{B_\phi + B_{SO}(1+\sqrt{1-\gamma^2})}\right) - \frac{1}{2\sqrt{1-\gamma^2}}\Psi\left(\frac{B}{B_\phi + B_{SO}(1-\sqrt{1-\gamma^2})}\right), \quad (1)$$

where $\Delta\sigma(B) = \sigma(B) - \sigma(0)$ is the correction to the conductance, $\sigma(B)$ is the magnetoconductance under magnetic field B, $G_0 = e^2/\pi h$ is the quantum of conductance, $\Psi(x)$ is defined as $\Psi(x) = \ln(x) + \psi(1/2+1/x)$, and $\psi(x)$ is the digamma function. The parameters in Eq. (1) are the inelastic field $B_\phi = \hbar/(4eD\tau_i)$ and the spin–orbit field $B_{SO} = \hbar/(4eD\tau_{SO})$.

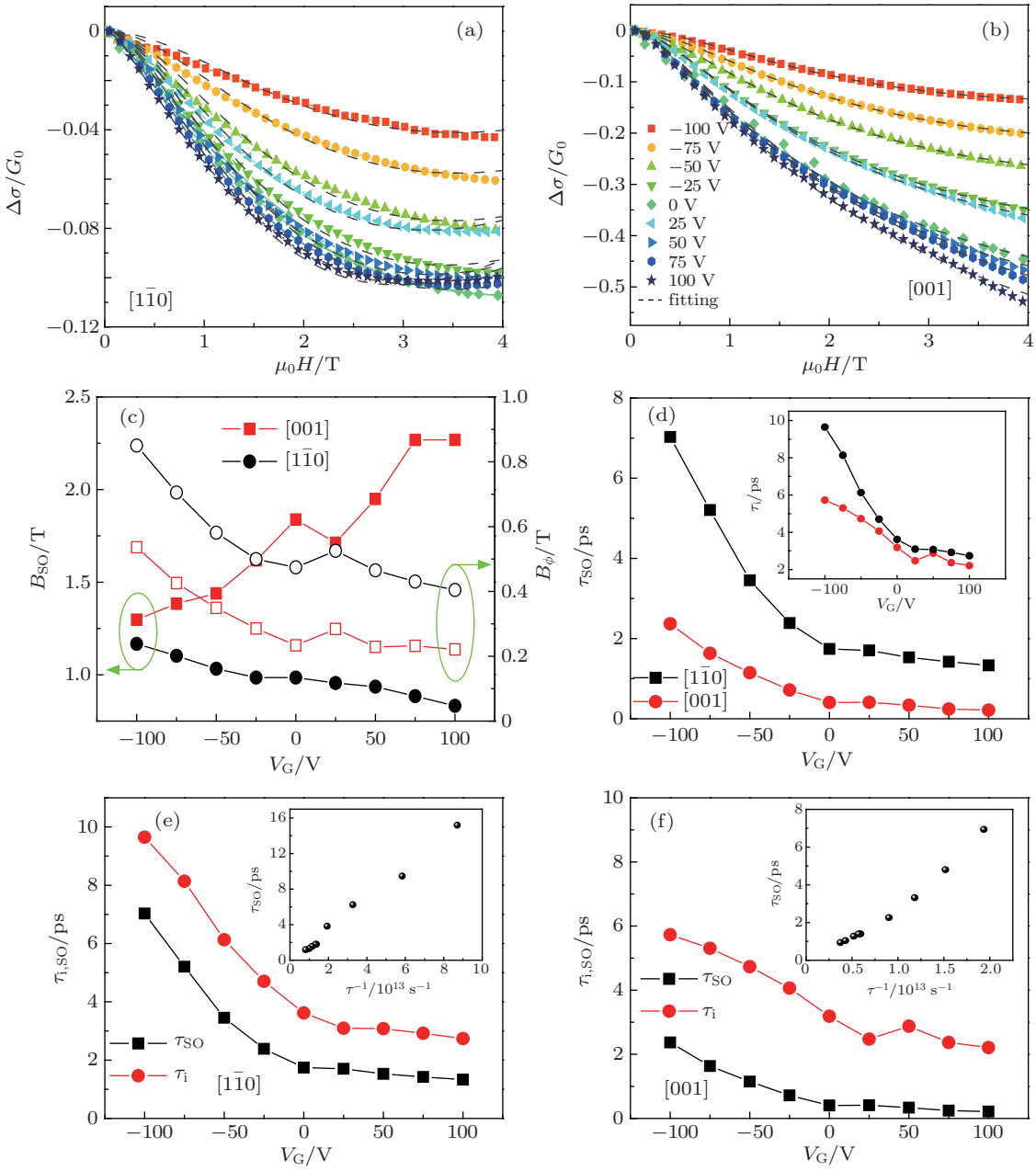


Fig. 4. (color online) The out-of-plane magnetoconductance (normalized by the quantum of conductance) at different V_G along (a) $[1\bar{1}0]$ and (b) [001] directions. The dark grey dashed lines are the fitting lines by using Eq. (1). (c) The obtained fitting parameters B_{SO} (filled square) and B_ϕ (open circle) as a function of V_G along $[1\bar{1}0]$ (black) and [001] (red) directions. (d) The τ_{SO} as a function of V_G along two directions, the inset shows the τ_i versus V_G. Comparing τ_{SO} with τ_i at different V_G along (e) $[1\bar{1}0]$ and (f) [001] directions. Spin relaxation time vs. elastic scattering rate along two directions is shown in the insets of panels (e) and (f). The lines are a guide to the eye.

The parameter $\gamma = g\mu_B B/4eDB_{SO}$ is the Zeeman correction factor in which g-factor enters, where μ_B is the Bohr magneton, $D = \pi\hbar^2 n_s \mu/(m^* e)$ is the diffusion constant, τ_i and τ_{SO} are the relaxation times related to inelastic and spin–orbit terms, respectively. n_s is the sheet carrier density and the effective mass of the electron takes $m^* = 3m_e$ at both directions.[29] It is worth mentioning that we also used the Hikami–Larkin–Nagaoka (HLN) formula.[23] to fit the experimental data. By fitting the temperature dependence of the magnetoconductance correction, the MF equation gives more reasonable parameters, especially the B_{SO}, compared with those of the HLN equation.

The evolution of the fitting parameters as a function of V_G is shown in Fig. 4(c). Along both directions, the inelastic field B_ϕ decreases as V_G increases. When increasing V_G, the sheet resistance decreases and the carrier density increases, so the inelastic scattering weakens. Along the $[1\bar{1}0]$ direction, with increasing V_G, the spin–orbit field B_{SO} decreases slightly, while along the [001] direction, the spin–orbit field increases as V_G increases. For both directions, the B_{SO} changes slightly with varying V_G. This insensitive gate tunable SOC may be attributed to the strong atomic orbital polarizations of d_{xy} and d_{xz}/d_{yz} orbitals along the confinement direction.[16] The corresponding scattering time as a function of V_G is shown in Fig. 4(d). Along both directions, τ_i decreases with increasing V_G, and τ_i is smaller than τ_{SO} (Figs. 4(e) and 4(f)), suggesting that the effect of the SOC is stronger compared with the orbital effect of the magnetic field. Moreover, a significant difference of spin–orbit term B_{SO} is observed. The τ_i is shorter along the $[1\bar{1}0]$ direction, suggesting that the weak localization is stronger than that of the [001] direction, which is consistent with the difference of sheet resistivity (Fig. 3(a)). For spin relaxation processes, there are mainly two typical scenarios: the Elliott–Yafet (EY) mechanism and the D'yakonov–Perel' (DP) mechanism.[30–32] In the latter mechanism, the spin relaxation time τ_{SO} is expected to be inversely proportional to the elastic scattering time τ. As shown in the insets of Figs. 4(e) and 4(f), τ_{SO} is proportional to the inverse of τ over a wide range of V_G, characterizing the Rashba spin–orbit interactions. Besides, we note a deviation for $V_G > 50$ V along the [001] direction, which may be due to the same order of τ and τ_{SO}. For intuitive comparison, all transport parameters for the sample prepared under the high oxygen pressure are listed in Tables 1 and 2.

Moreover, for the $P_{O2} = 10^{-4}$ Torr sample, down to mK magnitude of temperature, the superconductivity emerges, while for the $P_{O2} = 10^{-3}$ Torr sample, the superconductivity is absent. To our surprise, the superconductivity is anisotropic along the two directions, as shown in Fig. 5. The superconducting transition temperature (T_c) is lower but the out-of-plane critical field ($H_{c2,\perp}$) is larger along the $[1\bar{1}0]$ direction than that along [001] (inset of Fig. 5). The temperature dependence of $H_{c2,\perp}$ is extracted from the MR curves measured at different temperatures, where $H_{c2,\perp}$ is defined as the perpendicular magnetic field in which the sheet resistance of interfaces reaches to half of the normal state resistance taken at a given temperature. Generally, $H_{c2,\perp}$ should be proportional to T_c. We speculate that the unconventional larger $H_{c2,\perp}$ along the $[1\bar{1}0]$ direction is due to the effect of disorder.[33,34] The above MR results suggest the strong localization along the $[1\bar{1}0]$ direction. The deviation at low temperatures indicates that the effect of disorder overtakes the thermal fluctuation.[35] The mechanism of in-plane anisotropy of superconductivity needs further investigation and will be discussed elsewhere.

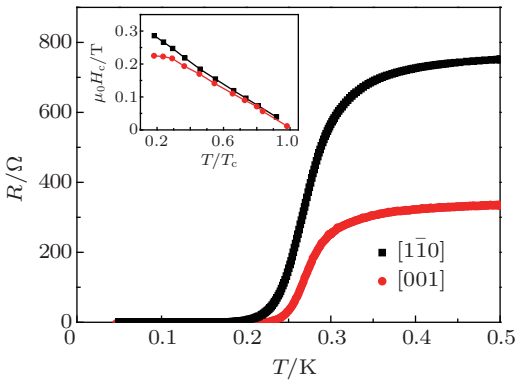


Fig. 5. (color online) Temperature dependence of the sheet resistance along two directions. The inset shows temperature dependence of the out-of-plane critical field, taken at 50% of normal resistance.

The anisotropic behavior along two directions $[1\bar{1}0]$ and [001] at the LAO/STO(110) interfaces may be due to the difference of Ti t_{2g} (i.e., d_{xy}, d_{yz}, and d_{zx}) orbitals. For LAO/STO(110), contrary to (001), the lower energy states have d_{yz}/d_{zx} character.[13] The ARPES results performed on $SrTiO_3$(110) surfaces reveal that the d_{yz}/d_{zx}-derived Fermi surface is anisotropic.[18] For the interface prepared at low P_{O2} (e.g., 10^{-4} Torr) , the carrier density is high (in our case, $\sim 6 \times 10^{13}$ cm^{-2}), and then both d_{xy} and d_{yz}/d_{zx} subbands are filled, the anisotropy weakens. However, for the interface prepared at high P_{O2} (e.g., 10^{-3} Torr), the carrier density is low ($\sim 2.2 \times 10^{13}$ cm^{-2}), only d_{yz}/d_{zx} derived ellipsoids appear, the anisotropy is obvious. Along the $[1\bar{1}0]$ direction, the d_{yz}/d_{zx} like subbands dispersing is weak and the effective electron mass is semiheavy, while the d_{yz}/d_{zx} like subbands dispersing is strong and the effective electron mass is light along the [001] direction.[17,18] The difference of d_{yz}/d_{zx} like subbands along the two directions may influence the properties of 2DEGs at the LAO/STO(110) interfaces.

4. Conclusion

We demonstrate the in-plane anisotropic behavior of 2DEG at LAO/STO(110) interfaces by performing magneto-transport and superconducting measurements. The anisotropy

becomes more obvious for samples of low carrier density. We find that the SOC is anisotropic and insensitive to the gate voltage, while the spin relaxation mechanism is the DP mechanism along both directions. The effect of localization is stronger along the $[1\bar{1}0]$ direction. Moreover, the anisotropic superconductivity is also observed, lower T_c but larger $H_{c2,\perp}$ is shown along the $[1\bar{1}0]$ direction. Such crystallographic tunable properties expand the possibilities for electronic engineering of two-dimensional electron gas at the $LaAlO_3/SrTiO_3$ interface.

References

[1] Brinkman A, Huijben M, Van Zalk M, Huijben J, Zeitler U, Maan J C, van der Wiel W G, Rijnders G, Blank D H and Hilgenkamp H 2007 *Nat. Mater.* **6** 493

[2] Reyren N, Thiel S, Caviglia A D, Kourkoutis L F, Hammerl G, Richter C, Schneider C W, Kopp T, Ruetschi A S, Jaccard D, Gabay M, Muller D A, Triscone J M and Mannhart J 2007 *Science* **317** 1196

[3] Caviglia A D, Gariglio S, Reyren N, Jaccard D, Schneider T, Gabay M, Thiel S, Hammerl G, Mannhart J and Triscone J M 2008 *Nature* **456** 624

[4] Bert J A, Kalisky B, Bell C, Kim M, Hikita Y, Hwang H Y and Moler K A 2011 *Nat. Phys.* **7** 767

[5] Dikin D, Mehta M, Bark C, Folkman C, Eom C and Chandrasekhar V 2011 *Phys. Rev. Lett.* **107** 056802

[6] Li L, Richter C, Mannhart J and Ashoori R C 2011 *Nat. Phys.* **7** 762

[7] Shalom M B, Sachs M, Rakhmilevitch D, Palevski A and Dagan Y 2010 *Phys. Rev. Lett.* **104** 126802

[8] Caviglia A, Gabay M, Gariglio S, Reyren N, Cancellieri C and Triscone J M 2010 *Phys. Rev. Lett.* **104** 126803

[9] Fête A, Gariglio S, Caviglia A, Triscone J M and Gabay M 2012 *Phys. Rev. B* **86** 201105

[10] Ohtomo A and Hwang H Y 2004 *Nature* **427** 423

[11] Annadi A, Zhang Q, Renshaw Wang X, Tuzla N, Gopinadhan K, Lu W M, Roy Barman A, Liu Z Q, Srivastava A, Saha S, Zhao Y L, Zeng S W, Dhar S, Olsson E, Gu B, Yunoki S, Maekawa S, Hilgenkamp H, Venkatesan T and Ariando 2013 *Nat. Commun.* **4** 1838

[12] Herranz G, Sanchez F, Dix N, Scigaj M and Fontcuberta J 2012 *Sci. Rep.* **2** 758

[13] Pesquera D, Scigaj M, Gargiani P, Barla A, Herrero-Martín J, Pellegrin E, Valvidares S, Gázquez J, Varela M and Dix N 2014 *Phys. Rev. Lett.* **113** 156802

[14] Herranz G, Bergeal N, Lesueur J, Gazquez J, Scigaj M, Dix N, Sanchez F and Fontcuberta J 2013 arXiv:1305.2411

[15] Han Y L, Shen S C, You J, Li H O, Luo Z Z, Li C J, Qu G L, Xiong C M, Dou R F, He L, Naugle D, Guo G P and Nie J C 2014 *Appl. Phys. Lett.* **105** 192603

[16] Herranz G, Singh G, Bergeal N, Jouan A, Lesueur J, Gazquez J, Varela M, Scigaj M, Dix N, Sanchez F and Fontcuberta J 2015 *Nat. Commun.* **6** 6028

[17] Gopinadhan K, Annadi A, Kim Y, Srivastava A, Kumar B, Chen J S, Coey J M D, Ariando and Venkatesan T 2015 *Adv. Electr. Matters* **1500114** 1

[18] Wang Z M, Zhong Z C, Hao X F, Gerhold S, Stoger B, Schmid M, Sanchez-Barriga J, Varykhalov A, Franchini C, Held K and Diebold U 2014 *Proc. Natl. Acad. Sci. USA* **111** 3933

[19] Shalom M B, Tai C, Lereah Y, Sachs M, Levy E, Rakhmilevitch D, Palevski A and Dagan Y 2009 *Phys. Rev. B* **80** 140403

[20] Komnik Y F, Andrievskii V V and Berkutov I B 2007 *Low Temp. Phys.* **33** 79

[21] Kawaguti T and Fujimori Y 1983 *J. Phys. Soc. Jpn.* **52** 722

[22] Spirito D, Di Gaspare L, Evangelisti F, Di Gaspare A, Giovine E and Notargiacomo A 2012 *Phys. Rev. B* **85** 235314

[23] Hikami S, Larkin A I and Nagaoka Y 1980 *Prog. Theor. Phys.* **63** 707

[24] Bergman G 1982 *Phys. Rev. Lett.* **48** 1046

[25] Lee P A and Ramakrishnan T V 1985 *Rev. Mod. Phys.* **57** 287

[26] Stornaiuolo D, Gariglio S, Fête A, Gabay M, Li D, Massarotti D and Triscone J M 2014 *Phys. Rev. B* **90** 235426

[27] Neville R C, Mead C A and Hoeneise B 1972 *J. Appl. Phys.* **43** 2124

[28] Maekawa S and Fukuyama H 1981 *J. Phys. Soc. Jpn.* **50** 2516

[29] Mattheiss L 1972 *Phys. Rev. B* **6** 4740

[30] Dyakonov M and Perel V 1972 *Soviet Physics Solid State USSR* **13** 3023

[31] Elliott R J 1954 *Phys. Rev.* **96** 266

[32] Yafet Y 1963 *Solid State Phys.* **14** 1

[33] Gurevich A, Patnaik S, Braccini V, Kim K H, Mielke C, Song X, Cooley L D, Bu S D, Kim D M, Choi J H, Belenky L J, Giencke J, Lee M K, Tian W, Pan X Q, Siri A, Hellstrom E E, Eom C B and Larbalestier D C 2004 *Supercond. Sci. Tech.* **17** 278

[34] Bugoslavsky Y, Cohen L, Perkins G, Polichetti M, Tate T, Gwilliam R and Caplin A 2001 *Nature* **411** 561

[35] Fisher D S, Fisher M P and Huse D A 1991 *Phys. Rev. B* **43** 130